Journal of Hazardous Materials 320 (2016) 581–590

Contents lists available at ScienceDirect

Journal of Hazardous Materials

journal homepage: www.elsevier.com/locate/jhazmat

pH-dependent degradation of *p*-nitrophenol by sulfidated nanoscale zerovalent iron under aerobic or anoxic conditions

Jing Tang[a,b], Lin Tang[a,b,*], Haopeng Feng[a,b], Guangming Zeng[a,b,*], Haoran Dong[a,b], Chang Zhang[a,b], Binbin Huang[a,b], Yaocheng Deng[a,b], Jiajia Wang[a,b], Yaoyu Zhou[a,b]

[a] College of Environmental Science and Engineering, Hunan University, Changsha 410082, China
[b] Key Laboratory of Environmental Biology and Pollution Control (Hunan University), Ministry of Education, Changsha 410082, China

HIGHLIGHTS

- The reactivity of NZVI towards PNP was remarkably enhanced after sulfidation.
- Anoxic S-NZVI systems preferred to weaker alkaline solutions, differing from NZVI.
- Aerobic S-NZVI systems performed better in acidic solutions, similar to NZVI.
- Degradation pathways of PNP under aerobic or anoxic conditions were proposed.

ARTICLE INFO

Article history:
Received 29 March 2016
Received in revised form 29 June 2016
Accepted 18 July 2016
Available online 29 July 2016

Keywords:
Sulfidation
Nanoscale zerovalent iron
Aerobic conditions
p-Nitrophenol
pH-dependent degradation

ABSTRACT

Sulfidated nanoscale zerovalent iron (S-NZVI) is attracting considerable attention due to its easy production and high reactivity to pollutants. We studied the reactivity of optimized S-NZVI (Fe/S molar ratio 6.9), comparing with pristine nanoscale zerovalent iron (NZVI), at various pH solutions (6.77–9.11) towards *p*-nitrophenol (PNP) under aerobic and anoxic conditions. Studies showed that the optimized extent of sulfidation could utterly enhance PNP degradation compared to NZVI. Batch experiments indicated that in anoxic S-NZVI systems the degradation rate constant increased with increasing pH up to 7.60, and then declined. However, in aerobic S-NZVI, and in anoxic or aerobic NZVI systems, it decreased as pH increased. It was manifested that anoxic S-NZVI systems preferred to weaker alkaline solutions, whereas aerobic S-NZVI systems performed better in acidic solutions. The highest TOC removal efficiency of PNP (17.59%) was achieved in the aerobic S-NZVI system at pH 6.77, revealing that oxygen improved the degradation of PNP by excessive amounts of hydroxyl radicals in slightly acidic conditions, and the TOC removal efficiency was supposed to be further improved in moderate acidic solutions. Acetic acid, a nontoxic ring opening by-product, confirms that the S-NZVI system could be a promising process for industrial wastewater containing sulfide ions.

1. Introduction

Zero valent iron (Fe(0)), in view of its low cost and accessibility, has been used to treat some toxic and refractory pollutants in the industrial wastewater, such as metals, organochlorine compounds, and nitroaromatic compounds [1–3]. Moreover, the environmentally physicochemical process motivated by Fe(0), based on the in-situ generation of Fe^{2+}, atomic hydrogen (•H, anoxic conditions) or hydroxyl (•OH, aerobic conditions) radicals [4–6], has attracted extensive attention. In detail, Fe(0) could be used to reduce heavy metal ions and reducible organic matters in water under anaerobic conditions [3,7]. And meanwhile, it is also a heterogeneous Fenton regent for advanced oxidation treatment of organic contaminants with abundance of oxygen [8]. Recent studies show that nanoscale zero valent iron (NZVI) could react with molecular oxygen to produce reactive oxygen species (ROS) which is able to oxidize or even mineralize organic contaminants [9]. However, there are some challenges to achieve successful implementation of this technology. For example, the formation of an iron oxide shell on NZVI reduces the reactivity [10]. A lot of studies have tried to improve the reactivity of NZVI in practical applications by: (i) immobilizing NZVI on polyporous supports to increase its reactivity towards the adsorbed compounds [11], (ii) coating NZVI with polymers to

* Corresponding authors at: College of Environmental Science and Engineering, Hunan University, Changsha 410082, China.
E-mail addresses: tanglin@hnu.edu.cn (L. Tang), zgming@hnu.edu.cn (G. Zeng).

http://dx.doi.org/10.1016/j.jhazmat.2016.07.042
0304-3894/

enhance the colloidal stability and increase its surface area available for reaction [12], and (iii) structuring bimetallic systems such as Fe/Pd, Fe/Au, Fe/Ni or Fe/Cu, where the electron transfer accelerates [13–17].

Recently, a few studies have reported that sulfide doped NZVI, produced by addition of dithionite ($Na_2S_2O_4$) during synthesis of NZVI via liquid phase reducing method or reaction between NZVI and sulfide ions, exhibited higher reactivity than pristine NZVI [18–20]. The generated iron sulfides, such as mackinawite and pyrite, exhibit a higher affinity for contaminants because of the hydrophobic nature and reducing capability [18,21]. Thus, electrons from iron tend to transfer to target compounds rather than water. Interestingly, many reports have shown that the electron availability at reactive surface increases at higher pH, and thus the reduction rate of TCE in FeS mediated NZVI systems clearly increases with increasing solution pH, opposite to the trend in NZVI systems [19,22]. Indeed, the increasing reactivity of nFe/FeS at higher pH levels was explained as follows. The hydrated FeS surface contains iron hydroxyl (≡FeOH) and bisulfide (≡SH) functional groups, and these groups undergo protonation ($\equiv FeOH + H^+ \leftrightarrow FeOH_2^+$) and deprotonation ($\equiv SH \leftrightarrow \equiv S^- + H^+$) reactions as the solution pH changes [22]. The difference in reactivity between negatively and positively charged surface species is that the negatively charged one is partly attributed to the greater driving force of deprotonated ligands in electron donation, which results in increased degradation at higher pH levels [23].

Furthermore, solution pH plays an important role in the production of reactive oxygen species (ROS) under aerobic conditions [24]. Specifically, the dissolved oxygen (DO) could be reduced into H_2O_2 in NZVI system through two-electron reactions (Equation (1) and (2)) [25], and then H_2O_2 would be transferred into $^{\bullet}OH$ radicals with the Fe^{2+} catalysis (Equation (3)). Under the neutral solution, H_2O_2 could be generated by the oxidation of primary product of Fe^{2+} with oxygen (Equation (4) and (5)) [25,26]. Subsequently, the ROS is formed through the Fenton reaction (Equation (3)). However, hydrous ferric oxides are produced under the alkaline conditions with few $^{\bullet}OH$ radicals forming (Equation (6)) [25,27]. Obviously, more $^{\bullet}OH$ radicals incline to be produced in Fe(0) systems at lower pH solutions under aerobic conditions.

$$Fe^0 + O_2 + 2H^+ \rightarrow H_2O_2 + Fe^{2+} \quad (1)$$

$$Fe^0 + H_2O_2 + 2H^+ \rightarrow Fe^{2+} + 2H_2O \quad (2)$$

$$Fe^{2+} + H_2O_2 \rightarrow {}^{\bullet}OH + Fe^{3+} + OH^- \quad (3)$$

$$Fe^{2+} + O_2 \rightarrow Fe^{3+} + {}^{\bullet}O_2^- \quad (4)$$

$$Fe^{2+} + {}^{\bullet}O_2^- + 2H^+ \rightarrow Fe^{3+} + H_2O_2 \quad (5)$$

$$4Fe^0 + 3O_2 + 6H_2O \rightarrow 4Fe(OH)_3 \quad (6)$$

According to the above mentioned, aerobic conditions and solution pH are rather important in the production of ROS. Although several studies have addressed the higher reactivity of sulfided NZVI than NZVI towards organic compounds and heavy metals in anoxic or anaerobic conditions, the reactivity of S-NZVI towards *p*-nitrophenol (PNP) in aerobic conditions has not been tested; neither do the reactivity of S-NZVI in different pH solutions. By the way, it has been reported that some noble metals such as Pd, Ag and Au may contribute to toxicity [28]. Sulfide ions, a prevalent substance in wastewater, can react with noble metal catalysts and reduce reactivity of NZVI. So it is an inevitable factor in evaluations of NZVI systems [29]. Hence, it is necessary to investigate the performance of sulfidated nanoscale zerovalent iron (S-NZVI) systems under aerobic and anoxic conditions for the practical applications. PNP, widely used as pesticides, polymers, pharmaceuticals and dye intermediates in industry or agriculture [30–32], serves as a model pollutant because of its reduced and oxidized abilities.

The objective of this study is to investigate the influence of oxygen on the reactivity of S-NZVI with varying pH. The reactivity of NZVI sulfidated to different extents for the treatment of PNP was optimized. The reactivity and TOC removal efficiency of S-NZVI systems were also compared with those of NZVI systems with varying pH (6.77–9.11) under anoxic or aerobic conditions to obtain the optimal technique and conditions for each system. Changes in surface mineral phase following sulfidation were characterized using TEM-Energy dispersive X-ray spectroscopy (TEM-EDS), X-Ray Diffraction (XRD) and X-ray photoelectron spectroscope (XPS). Changes in surface charge and KA_{ow} of NZVI and S-NZVI were also measured. The mechanism of PNP degradation under anoxic or aerobic conditions was proposed by analyzing the variation in FTIR spectra, X-ray photoelectron spectra and the intermediates with gas chromatography–mass spectrometry (GC–MS) after the treatment, combined with the capture of active species tests.

2. Experimental

2.1. Chemical reagents and preparation of S-NZVI

The regents used and NZVI are presented in S1 of Supporting information (SI). The preparation procedure of S-NZVI is described in S2 of SI, and the characterization methods are mentioned in S3 of SI.

2.2. Batch experiments

Preliminary experiments for optimizing Fe/S molar ratios of S-NZVI were described in S4 of SI. Besides, PNP degradation experiments were performed with two parameters as follows: (i) in a borate buffer adjusted to pH 6.77, 7.60, 8.41 or 9.11 (0.05 M sodium borate solution adjusted with 0.2 M boric acid solution containing 0.05 M NaCl); (ii) air aeration (aerobic conditions) or purging with N_2 (anoxic conditions). The inorganic buffer was chosen because of its weak interaction with ferrous ions in solution [33]. In addition, the purging rate was set up at 1 L/min referring to previous studies [4]. All analytical procedures for determination of the residual concentration of PNP, TOC, H_2O_2, iron speciation, sulfide ions, sulfate ions, main intermediates (*p*-aminophenol and *p*-benzoquinone) and identification of intermediates were described in S5 of SI.

3. Results and discussion

3.1. Characterization of NZVI and S-NZVI particles

The NZVI and S-NZVI materials were characterized by TEM coupled with EDS for analysis and elemental mapping. Similar to other studies [20,34], Fig. 1a and b show that both of pristine NZVI and S-NZVI particles with oxide shell aggregate with an average size approximately 50 nm. However, the shell for S-NZVI at the Fe/S molar ratios of 6.9 is much rougher than pristine NZVI particles' on account of the sulfidation. EDS measurements of NZVI samples showes peaks for Fe as well as inevitable C and O (Fig. 1a), whereas Fig. 1b about S-NZVI showes the peak for S demonstrating the presence of S upon sulfidation. Furthermore, the elemental mapping of S-NZVI (Fig. 1c) confirmed that S element was highly dispersed on NZVI particles.

Zeta potential of NZVI and S-NZVI particles were determined in a wide range of pH (from 3 to 9), and the corresponding results are presented in Fig. S1. The isoelectric points (pHzpc) for NZVI and S-NZVI occurred at pH 6.8 and 5.8, respectively. The descending pHzpc after the incorporation with S element suggestes that the surface of NZVI was coated with iron sulfide [22]. In addition, the XRD spectra of S-NZVI (shown in Fig. S2) demonstrated the exis-

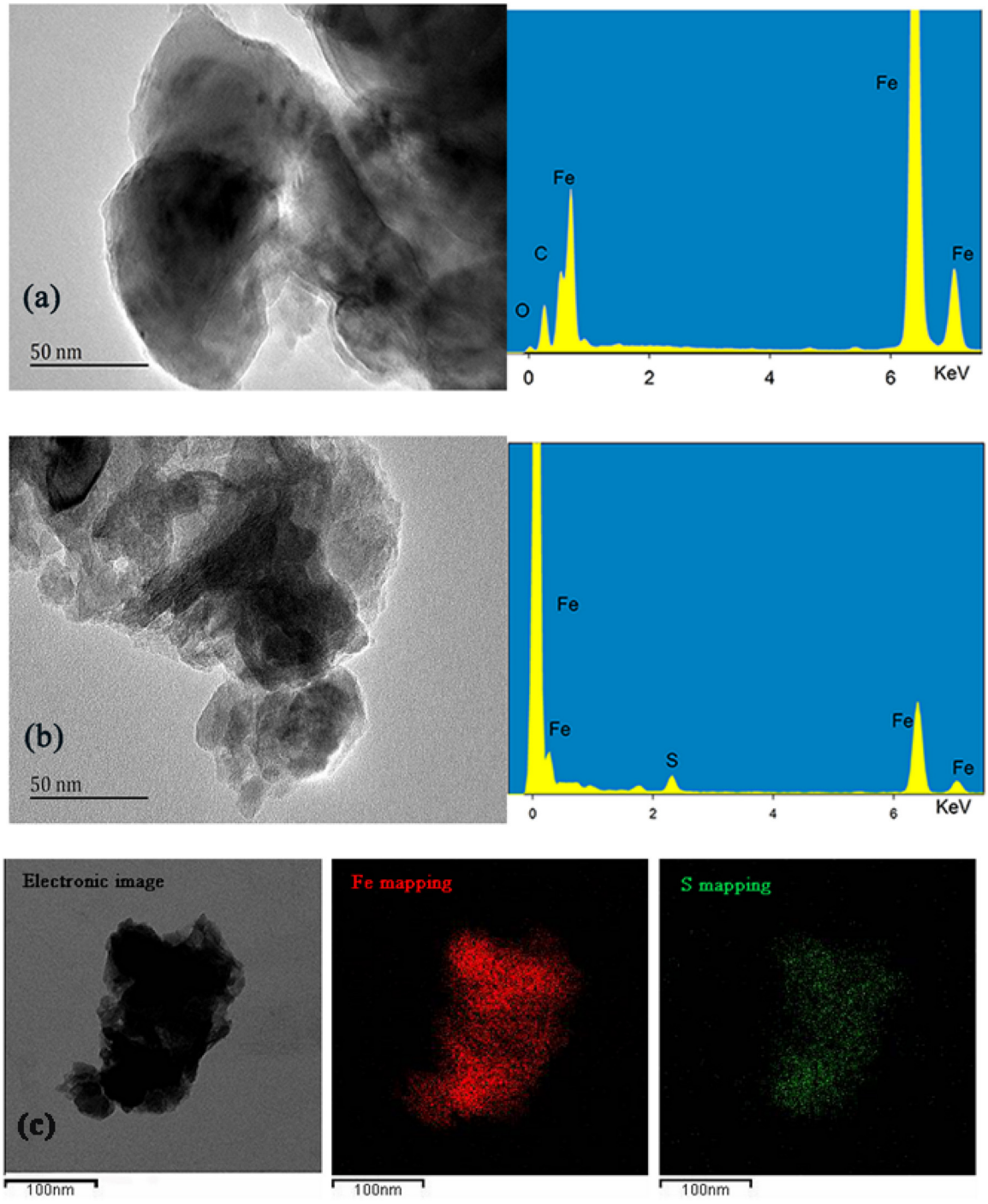

Fig. 1. TEM images and EDS spectra for pristine NZVI (a) and NZVI sulfidated at Fe/S of 6.9 (b), and elemental mapping images (c) of the S-NZVI for Fe and S from the electronic image.

tence of Fe(0) and Fe_3O_4. Due to the low level of S element, XRD could not detect the S element, so FeS_2 or FeS was hardly obtained directly by using XRD.

3.2. PNP degradation by S-NZVI or NZVI particles

Fig. 2 shows the degradation of PNP in 0.32 mg/L slurries of NZVI modified with sulfide ions at various concentrations. Compared to the pristine NZVI, S-NZVI obviously promoted the degradation for PNP. Its degradation rate increased with increasing doses of sulfide at Fe/S ratio from 20.68 to 6.9. Nevertheless, the PNP degradation rate decreased slightly with higher doses of sulfide at Fe/S ratio of 5.7. Thus, S-NZVI with Fe/S ratio of 6.9 was applied to investigate the reaction mechanism in various pH solutions under anoxic or aerobic conditions.

It has been reported that iron sulfides on the surface of iron conduct delocalized electrons in its planar layer [23]. What's more, Parket al., suggested that sulfide minerals were less hydrophilic compared to iron oxides [21]. Sai Rajasekar C. inferred that the FeS layer on the S-NZVI enhanced local binding of TCE and conducted more electrons to TCE rather than water molecules compared to pristine NZVI [19]. We compared the availability factor of

Table 1
The availability factor of electrons generated from S-NZVI or NZVI for reduction product (*p*-aminophenol) under anoxic conditions at the initial stage ($C_{electron} = 2 \times C_{Fe}^{2+} + 3 \times C_{Fe}^{3+}$).

Materials	$C_{p\text{-aminophenol}}$ (mM)	C_{Fe}^{2+} (mM)	C_{Fe}^{3+} (mM)	$C_{electron}$ (mM)	$C_{p\text{-aminophenol}}/C_{electron}$
S-NZVI	0.37	0.64	0.010	1.31	0.28
NZVI	0.30	0.70	0.007	1.42	0.21

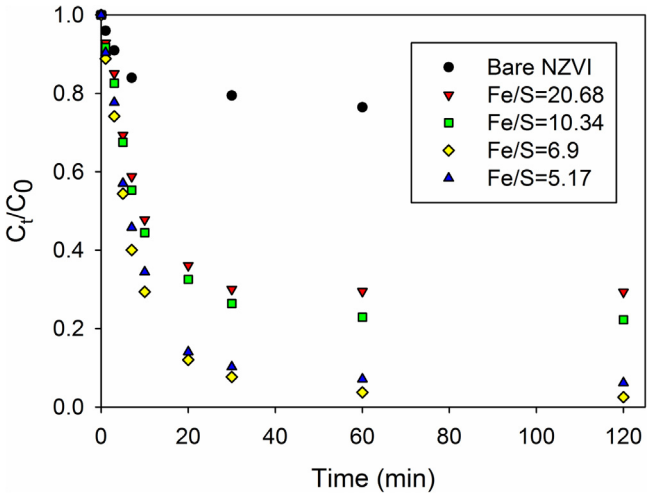

Fig. 2. Comparisons of PNP degradations (C_t/C_0 representing for the residual concentration of PNP at treatment time t (min) divided by the initial concentration) in unbuffered pH sealed systems containing S-NZVI with different Fe/S molar ratios or pristine NZVI at 0.32 mg/L, with initial PNP concentration of 0.72 mM and temperature at 25 ± 2 °C. All the standard deviations were less than 0.05.

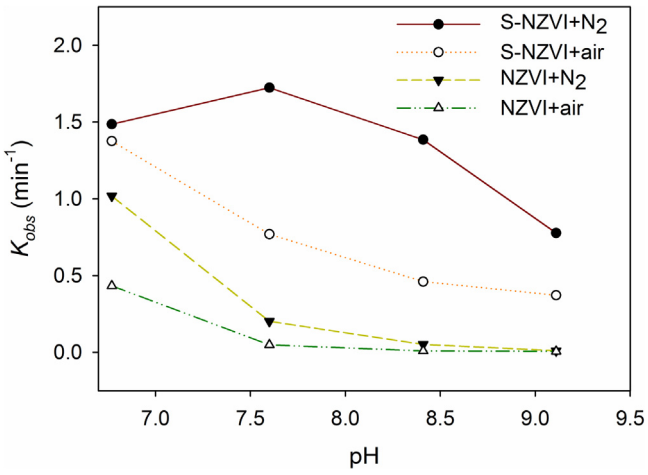

Fig. 3. Apparent PNP degradation rate constants for 0.32 mg/L optimized S-NZVI or NZVI systems with various buffered pH (6.77, 7.60, 8.41 and 9.11) purging with N_2 or air with initial PNP concentration of 0.72 mM, temperature at 25 ± 2° C and contact time of 60 min. All the standard deviations were less than 0.05.

electrons generated from S-NZVI or NZVI for reduction product (*p*-aminophenol) under anoxic conditions at the initial stage. These data was obtained at reaction time of 1 min, because at the stage, the precipitation of iron ions was negligible. In anoxic conditions, the oxygen oxidation also can be neglected. As shown in Table 1, the availability factor of electrons was calculated.as the equation $C_{electron} = 2 \times C_{Fe}^{2+} + 3 \times C_{Fe}^{3+}$. The higher factor indicates that the more electrons generated from materials were used to reduce PNP to *p*-aminophenol. Obviously, the factor of S-NZVI was higher than that of NZVI. It demonstrated that more electrons generated from S-NZVI were conducted to nitro groups of PNP. On the other hand, the pristine NZVI preferentially conducted electrons to water. However, an increase in sulfidation beyond the optimal dose range caused higher amount of FeS_2 formed on the surface, which reduced the reactivity [35]. The lower reactivity of NZVI sulfidated at Fe/S ratio of 20.68 might be attributed to incomplete coverage of the NZVI surface by FeS. The optimal Fe/S ratio is 6.9 lower than the appropriate value ranging from 12 to 25 described in Rajasekar C's studies [19]. Rajasekar C proved that the wash could release sulfide ions and the reactivity of S-NZVI above the optimal dose range would increase after wash. So, the lower optimal ratio obtained in our study might be due to the loss of sulfide ions by the wash in material preparation. During the wash process, the concentration of sulfide ions in the ultrapure water containing resultant S-NZVI still reached 0.02 mM, and some sulfide ions inevitably were oxidized to sulfate ions during the preparation process (Table S1), which proved the hypothesis.

3.3. *Degradation kinetics for buffered aqueous PNP in S–NZVI or NZVI systems under aerobic and anoxic conditions*

In Section 3.2, it was found that the reactivity of S-NZVI was much higher than that of Fe(0) under the sealing conditions. In this Section, the reactivities of S-NZVI and pristine NZVI for buffered PNP solutions (0.72 mM) at different pH values was investigated under aerobic and anoxic conditions. As shown in Fig. S3, the PNP removal equilibrium reached within a few minutes. Hence, kinetic model was applied to estimate the degradation mechanism in the initial stage. Due to the solid-liquid inter-phase reaction, the pseudo-first-order was utilized to fit the experimental data [30]. The kinetic rate equation is expressed in Equation (7).

$$\ln \frac{C_t}{C_0} = -K_{obs} t \quad (7)$$

where C_t and C_0 (mg/L) are the residual concentration of PNP at treatment time t (min) and the initial concentration, respectively; K_{obs} (min^{-1}) is the apparent rate constant, which is calculated by the method of linear regressions.

A plot of natural logarithmic C_t/C_0 versus the treatment time t is shown in Fig. S4, and the values of the constant K_{obs} and correlation coefficients R^2 were calculated and given in Table 2. A good linear fitting was observed in each of the batch experiments ($R^2 > 0.90$).

In order to intuitively compare PNP degradation rates under different conditions, Fig. 3 shows the K_{obs} versus the buffered solution pH values under aerobic and anoxic conditions. No matter under which conditions, it was clear that the K_{obs} obtained in S-NZVI systems were obviously higher than those obtained in NZVI systems at pH from 6.77 to 9.11. Under the anoxic and aerobic conditions, the K_{obs} (1.724 and 0.769 min^{-1}) obtained in S-NZVI systems were approximate 9 and 16 times higher than those (0.201 and 0.0479 min^{-1}) obtained in NZVI systems at pH 7.60, respectively. The results could be explained in two main aspects. (a) As the corrosion rate of NZVI was low in a slightly alkaline solution, •H was hard to be generated to reduce the pollutants under anoxic conditions. As shown in Fig. 4, at the beginning of reactions (first 3 min) when the precipitation of iron ions was negligible, the sum of Fe^{2+} and Fe^{3+} molarities in S-NZVI or NZVI systems with pH 6.77 was higher than that in systems with pH 7.60, which demonstrated that the corrosion rate of NZVI or S-NZVI was lower in more alkaline solutions. Meanwhile, the DO also could not obtain enough electrons

Table 2
Pseudo-first-order model parameters for PNP removal in S-NZVI and NZVI systems under different aeration and solution pH conditions.

Samples	Condition	Solution pH	Apparent rate constant (K_{obs})	Correlation coefficients (R^2)
S-NZVI	Purging with N_2	6.77	1.486	0.98
		7.60	1.724	0.96
		8.41	1.385	0.98
		9.11	7.77×10^{-1}	0.98
	Air aeration	6.77	1.376	0.92
		7.60	7.69×10^{-1}	0.96
		8.41	4.60×10^{-1}	0.93
		9.11	3.71×10^{-1}	0.98
NZVI	Purging with N_2	6.77	1.018	0.99
		7.60	2.01×10^{-1}	0.98
		8.41	5.08×10^{-2}	0.95
		9.11	1.01×10^{-2}	0.90
	Air aeration	6.77	4.33×10^{-1}	0.98
		7.60	4.79×10^{-2}	0.94
		8.41	8.30×10^{-3}	0.90
		9.11	5.50×10^{-3}	0.96

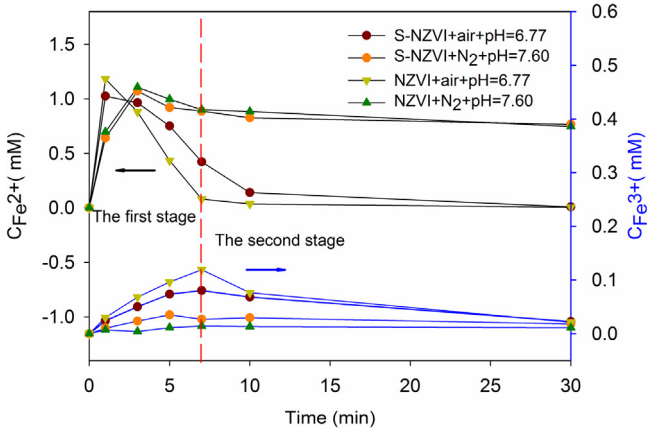

Fig. 4. Concentrations of Fe^{2+} and Fe^{3+} under purging with N_2 (pH 7.60) or air treatment (pH 6.77) by S-NZVI or NZVI with initial PNP concentration of 0.72 mM, temperature at 25 ± 2 °C and contact time of 30 min, all the standard deviations less than 0.05.

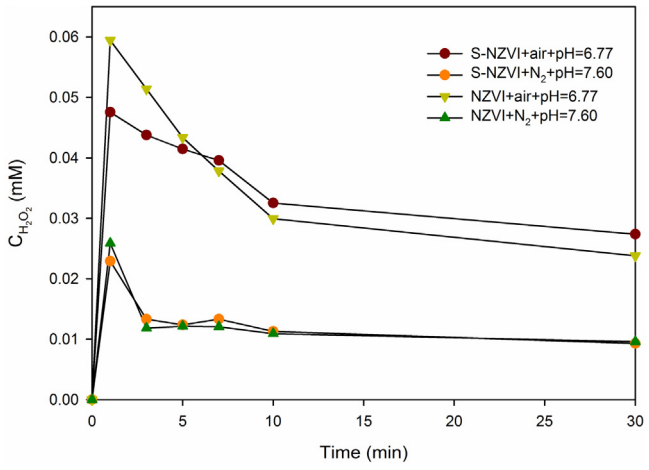

Fig. 5. Concentrations of H_2O_2 under purging with N_2 (pH 7.60) or air treatment (pH 6.77) by S-NZVI or NZVI with initial PNP concentration of 0.72 mM, temperature at 25 ± 2 °C and contact time of 30 min, all the standard deviations less than 0.05.

Table 3
KA_{ow} of NZVI and S-NZVI materials.

Material	NZVI	S-NZVI
KA_{ow} (Mean ± 95%C.L.)	1.37 ± 0.21	2.25 ± 0.16

from NZVI to generate H_2O_2 under aerobic conditions, and then the generated Fe^{2+} was almost all oxidized into Fe^{3+} (Equation (8)).

$$Fe^{2+} + 1/2H_2O + 1/4O_2 \rightarrow Fe^{3+} + OH^- \quad (8)$$

At the initial stage (in Fig. 4) of aerobic reaction, the molarity of Fe^{3+} increased obviously, while the decline of Fe^{3+} might be attributed to the precipitation of large amounts of iron ions. (b)FeS layers on the S-NZVI made iron particles more hydrophobic [19,21], KA_{ow} values greater than 1 indicate a hydrophobic material, and larger values indicate higher hydrophobic properties [36]. As shown in Table 3, the KA_{ow} value of S-NZVI is nearly twice as large as that of NZVI, which determines that S-NZVI is more hydrophobic than NZVI. Thus, the introduction of FeS would cause effective electron transfers from S-NZVI to hydrophobic nitro groups of PNP and oxygen molecules. Consequently, in S-NZVI systems, the formed •H radicals are able to reduce PNP under anoxic conditions, while excessive amounts of H_2O_2 and •OH radicals are generated under aerated conditions (eqution (1) and (3)). For these reasons, the reactivity of S-NZVI was much higher than that of NZVI particles.

In S-NZVI systems, the resulting K_{obs} under anoxic conditions at pH 7.60 was higher than that in a slightly acidic solution at pH 6.77, and subsequently the PNP degradation rate constant significantly decreased from 1.724 min^{-1} to 0.777 min^{-1} with increasing solution pH from 7.60 to 9.11. A lot of papers showed that the rate of electron transfer reactions of S-NZVI was faster at higher pH values due to the larger negative surface charge, resulting in the enhanced degradation of PNP in slightly alkaline solutions [19,22]. Due to the pKa (7.15) of PNP, while solution pH increased to alkaline, PNP molecules were gradually ionized into PNP anions, and the net charge on the surface of S-NZVI was negative [37]. Especially in solutions at pH up to 7.60, electrostatic repulsions played a more important role in the degradation, so the degradation rate decreased. However, under aerobic conditions, the PNP degradation rate in S-NZVI and NZVI dropped with the increasing solution pH from 6.77 to 9.11. The phenomenon can be explained by that generated H_2O_2 and •OH radicals were insufficient to remove PNP because of lacking H^+ and Fe^{2+} under alkaline conditions [24]. Fig. 5 shows that the concentrations of H_2O_2 in pH 6.77 solutions was much higher than that in pH 7.60 solutions, which revealed that acid environment is conductive to the formation of H_2O_2. What's more, the surface of particles would be covered by iron oxide hydroxide that could hinder electron transfers to a certain degree [10], accompanied with the electrostatic repulsions, and thus the PNP removal dramatically decreased, which also accounted for the

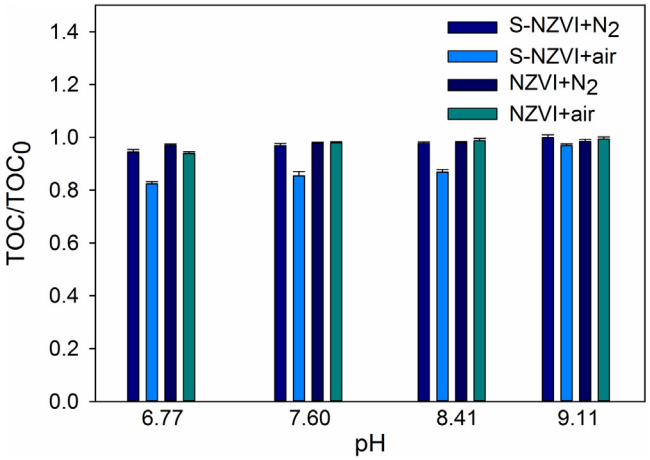

Fig. 6. TOC removal efficiency of PNP in 0.32 mg/L optimized S-NZVI or NZVI systems with various buffered pH values after 60 min treatment purging with N_2 or air, with initial PNP concentration of 0.72 mM and temperature at 25 ± 2 °C, errors bars indicating standard deviations.

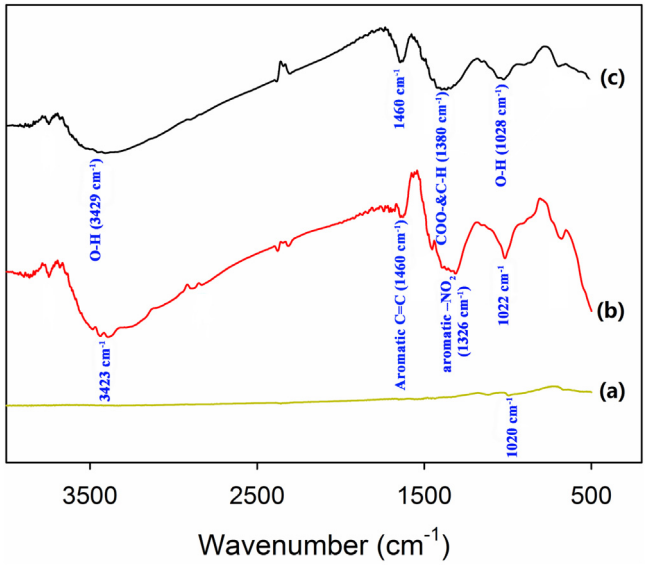

Fig. 7. The FITR spectra of S-NZVI before (a) and after reacting 0.72 mM PNP under purging with N_2 (b) or air (c) conditions.

descending PNP degradation rate with the increasing solution pH in NZVI systems in anoxic conditions.

It was a remarkable fact in S-NZVI systems that the K_{obs} at pH 6.77 dealing with the aerobic conditions was just lower than that under anoxic conditions. It manifested that aerobic treatment made S-NZVI produced excessive amounts of H_2O_2 and •OH radicals to degrade PNP under the slightly acidic solution in presence of adequate H^+ and Fe^{2+}, and the degradation efficiency was improved.

3.4. The influence of experimental conditions on TOC removal of PNP in S-NZVI and NZVI systems

Fig. 6 shows the plots of TOC/TOC_0 after 60 min treatment versus the buffered solution pH values under anoxic and aerobic conditions. The TOC removal of PNP under aerobic conditions was more obvious than that in anoxic conditions no matter in S-NZVI or NZVI systems. The phenomenon could be explained by the theory that the benzene ring of PNP could not opened under anoxic conditions, while in aerobic conditions the cleavage of benzene ring of PNP as well as its TOC removal by the generated •OH radicals occurred [4]. Obviously, TOC removal decreased with the increasing solution pH values, indicating that H^+ might play an indispensable role in production of •OH radicals. Especially, on account of the higher reactivity of S-NZVI, the highest TOC removal efficiency of PNP reached 17.59% in the S-NZVI system at pH 6.77 under aerobic conditions. The elevated efficiency of TOC removal in aerobic conditions was mainly attributed to oxidative degradation with the help of adequate oxygen. In Section 3.3, acid solutions was proved that a larger amount of H^+ in moderate acidic solutions has the potential to promote the yield of H_2O_2. What's more, in our previous studies [10], at solution pH lower than 3, the concentration of H^+ was so high that H^+ reacted with NZVI directly to produce hydrogen, which inhibited the PNP degradation reaction to a certain degree. Similarly, strong acid environment could boost the formation of hydrogen and then reduce the amount of electrons which intend to transfer to oxygen molecules, which means that the strong acid solution might not be suitable for the production of H_2O_2 by NZVI and S-NZVI. For these reasons, the TOC removal efficiency of PNP was supposed to be further improved in moderate acidic solutions.

3.5. FTIR spectral and XPS analysis

To gain further insights into the PNP degradation mechanism on S-NZVI under different conditions, the FTIR technique was used to analyze the exhausted materials. Fig. 7 shows the FTIR adsorption spectra of the S-NZVI before and after reaction dealing with the aerobic conditions or purging with nitrogen. The FTIR spectrum of unused S-NZVI (Fig. 7a) displays the weak band (1020 cm^{-1}), which is attributed to the stretching vibration of O—H and hydrogen-bonded O—H [38]. The FTIR spectrum of the reacted S-NZVI purging with nitrogen is shown in Fig. 7b. Particularly, the broad and intense band at 3423 cm^{-1} and the band at 1022 cm^{-1} are regarded to the stretching vibration of O—H and hydrogen-bonded O—H [4]. The band located at 1640 cm^{-1} is assigned to aromatic C=C skeletal vibrations [39,40]. In addition, the band observed at 1326 cm^{-1} is attributed to the aromatic —NO_2 symmetrical stretching vibration [4]. Fig. 7c is the FTIR spectrum of the reacted S-NZVI dealing with aeration. The spectrum shows some similar peaks (3429, 1460, 1028 cm^{-1}) to those shown in Fig. 7b. However, the emerging band at 1380 cm^{-1} corresponds to COO— antisymmetric stretching or C—H bending of CH_2 and CH_3 groups [39], which indicates that chain organic matters are generated, and the ring-opening reaction of PNP can occur in S-NZVI systems in aerobic conditions.

Table 4
The percentage composition of each element in various materials.

Element compositions (atomic%)	C	O	Fe	S	N
NZVI	40.72	47.90	11.37	–	–
S-NZVI	34.84	47.36	15.53	2.27	–
S-NZVI after purging with N_2	25.26	57.96	17.97	0.38	0.42
S-NZVI after air aeration	28.92	57.54	12.28	0.44	0.81

Moreover, X-ray photoelectron spectroscopy (XPS) was also applied to study the surface chemical compositions of the newly synthesized and treated samples for comparison. Semiquantitative compositions of NZVI, S-NZVI before interaction and S-NZVI after PNP removal dealing with the aerobic conditions or purging with nitrogen were calculated by the Software Avantage (Table 4). Even though precautions were taken during the synthesis and preparation of samples for analysis, it was impossible to completely eliminate oxygen that adsorbed at the surface. Besides, carbon was an unavoidable contaminant [41]. The presence of S at the S-NZVI sample surface demonstrated that S element had been fixed on NZVI particles. After contact with PNP for 1 h under anoxic or aerobic conditions, the new appearance of N stated the attachment of PNP and its intermediates to S-NZVI. Impressively, the S content of

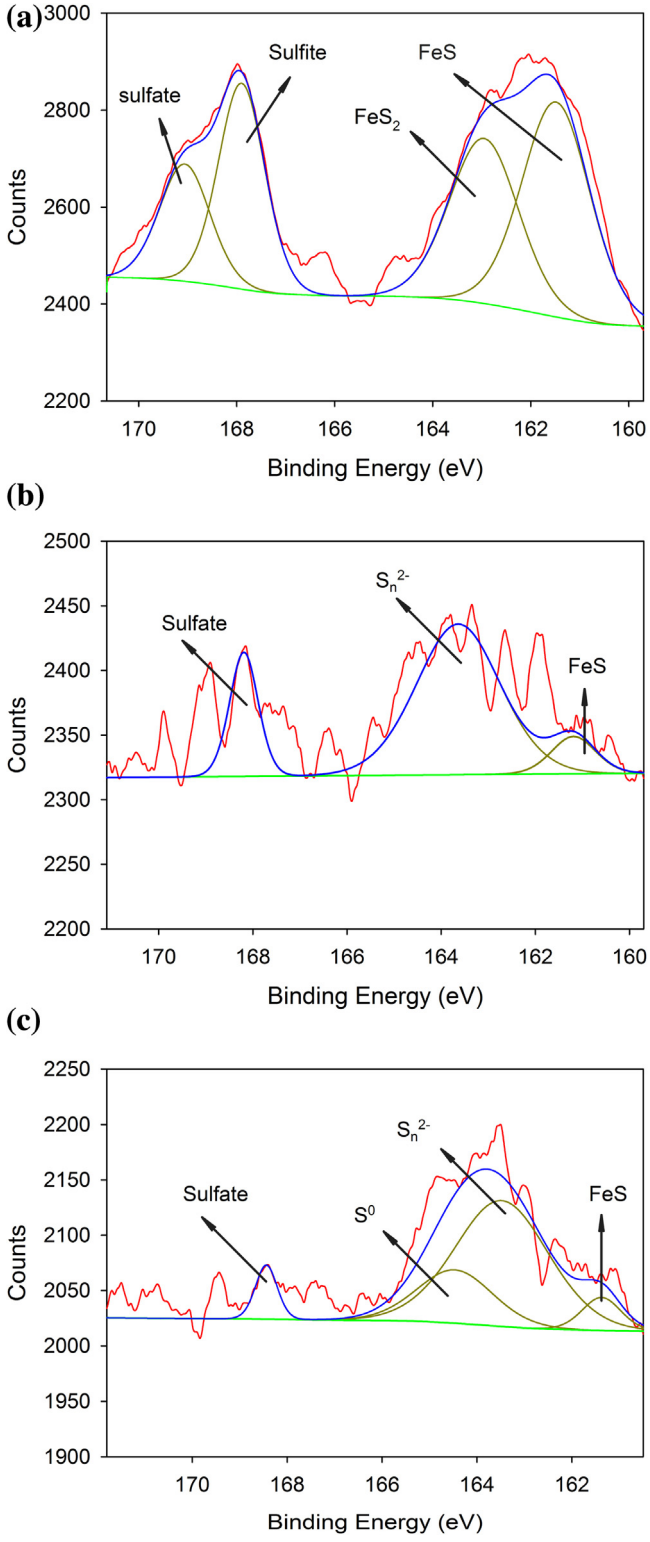

Fig. 8. Detailed XPS survey of the region for S(2p) for S-NZVI before (a) and after reacting 0.72 mM PNP under purging with N_2 (b) or air (c) conditions.

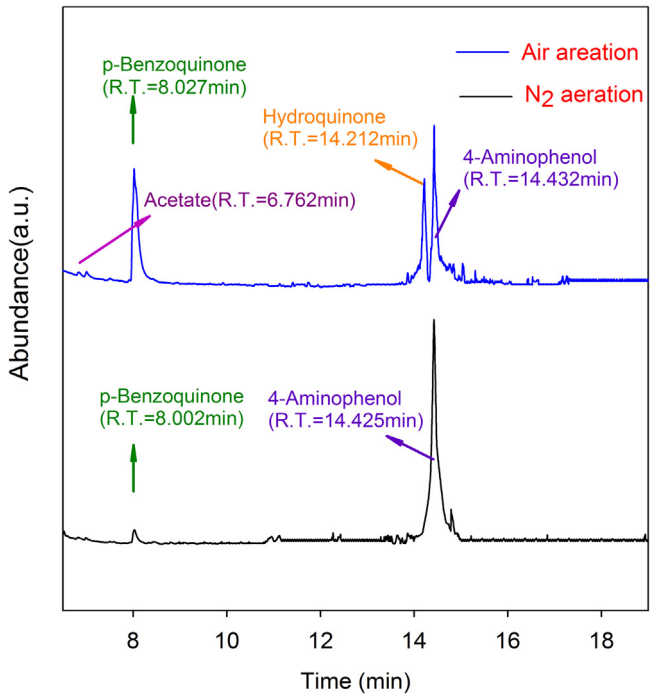

Fig. 9. GC–MS chromatograms on dichloromethane extract from the effluent after 60 min reactions under purging with N_2 or air treatment by S-NZVI.

used S-NZVI nearly decreased by an order of magnitude. Furthermore, as shown in Table S1, the concentrations of sulfide ions and sulfate ions in the two solutions after reactions under anoxic or aerobic conditions were both increased to different extents compared to the concentrations before reactions. It could be concluded that S-NZVI might release sulfide into water or air phase during the interaction with PNP.

The narrow region spectra for S(2p) and Fe(2p) are respectively shown in Fig. 8 and Fig. S5. To adequately fit the S(2p) spectrum of S-NZVI (Fig. 8a), four major fitting peaks were required. The peak with binding energy at 161.4 ± 0.3 eV, representing the main S(2p) signal, is typically assigned to FeS, and that at 163.1 ± 0.3 eV is attributed to FeS_2 [19,42]. Additionally, the other two peaks located at 167.9 and 169.0 eV are corresponded to sulfite and sulfate, respectively [43]. The existence of sulfite and sulfate reveals that some oxidation of the surface may have occurred before the PNP treatment. As for S(2p) spectra of the S-NZVI sample treated under anoxic conditions (Fig. 8b) or aerobic conditions (Fig. 8c), similar to Fig. 8a, there are still two weaker peaks attributed to FeS and sulfate. The presence of the strongest peak at 163.4 eV (shown in Fig. 8b and c), supposed to polysulfides S_n^{2-} species [41], indicates that PNP degradation process stimulates FeS to be oxidized into polysulfides species. The particular peak at 164.4 eV corresponding to S_0 discloses that the extent of oxidation under aerobic conditions is greater than that under anoxic conditions because of the additional oxygen [44].

As shown in Fig. S5a and S4b, peaks of pristine NZVI and S-NZVI show the presence of Fe(II), Fe(III) and Fe(0), corresponding to the results of XRD analysis. Notably, the peak for Fe(0) of S-NZVI is weaker than that of NZVI, which might result from oxidation during the sulfide-modified preparation. As for the Fe(2p) spectra of these used S-NZVI (shown in Fig. S5c and S5d), the disappearance of the peak for Fe(0) testifies that the oxidation of the surface Fe(0) happened in degradation processes, consistent with the conclusion gained from Fig. 8.

3.6. Roles of active species in PNP degradation under anoxic and aerobic conditions

In spite of the theory that the active species (•OH radicals) may exist in PNP degradation process, there is no definite evidence to confirm the presence of that active species. Otherwise, the familiar active oxygen species ($^{\bullet}O_2^-$) is also likely to show up (Equation

Table 5
Comparisons of pseudo-first-order model parameters for PNP removal in S-NZVI systems with an addition of scavengers, *n*-butanol or *p*-benzoquione.

Condition	Solution pH	Scavenger	Apparent rate constant (K_{obs})	Correlation coefficients (R^2)
Purging with N_2	7.60	None	1.724	0.95
	7.60	*N*-butanol	1.563	0.93
	7.60	*P*-benzoquione	1.705	0.88
Air aeration	6.77	None	1.376	0.92
	6.77	*N*-butanol	1.048	0.92
	6.77	*P*-benzoquione	1.294	0.83

(4)). Therefore, in S-NZVI systems at pH 6.77 under anoxic and aerobic conditions, roles of those active species in PNP degradation were studied by •OH radicals scavenger and $^{\bullet}O_2^-$ scavenger. Table 5 compares pseudo-first-order model parameters for PNP removal in S-NZVI systems with an addition of scavengers.

•OH radicals are very short-lived active species, and some scavengers, such as *n*-butanol, isopropanol and salicylic acid, were commonly employed to indirectly characterize its roles in pollutants degradation [45]. As shown in Table 5, the addition of *n*-butanol with 0.01 mM into the anoxic system made the K_{obs} decline to 11.9% (from 1.774 to 1.563 min^{-1}), while the K_{obs} decreased to 23.8% (from 1.376 to 1.048 min^{-1}) in the aerobic systems. These results suggested that •OH radicals played a more important role in PNP degradation under aerobic conditions than that under anoxic conditions. A small amount of generation of •OH radicals in anoxic system might be ascribed to unavoidable residual oxygen.

Under the neutral solution, H_2O_2 also could be generated from the oxidation of S-NZVI by oxygen can also generate the important intermediate, $^{\bullet}O_2^-$ with no H^+ ions consumed in the reaction (Equation (5)). P-benzoquinone was used to capture $^{\bullet}O_2^-$ [46]. The effect of *p*-benzoquinone on PNP degradation in the anoxic and aerobic systems was evaluated and shown in Table 5. The presence of *p*-benzoquinone exhibited a negligible negative role in PNP degradation, revealing that $^{\bullet}O_2^-$ had slight impacts on PNP degradation in the buffered solution at pH 6.77 under anoxic and aerobic conditions, and H_2O_2 was primarily generated by Equation (1).

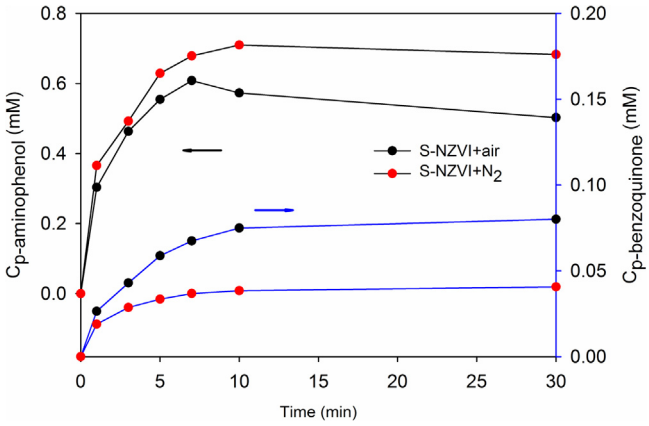

Fig. 10. Concentrations of *p*-aminophenol and *p*- benzoquinine under purging with N_2 (pH 7.60) or air treatment (pH 6.77) by S-NZVI with initial PNP concentration of 0.72 mM, temperature at 25 ± 2 °C and contact time of 30 min, all the standard deviations less than 0.05.

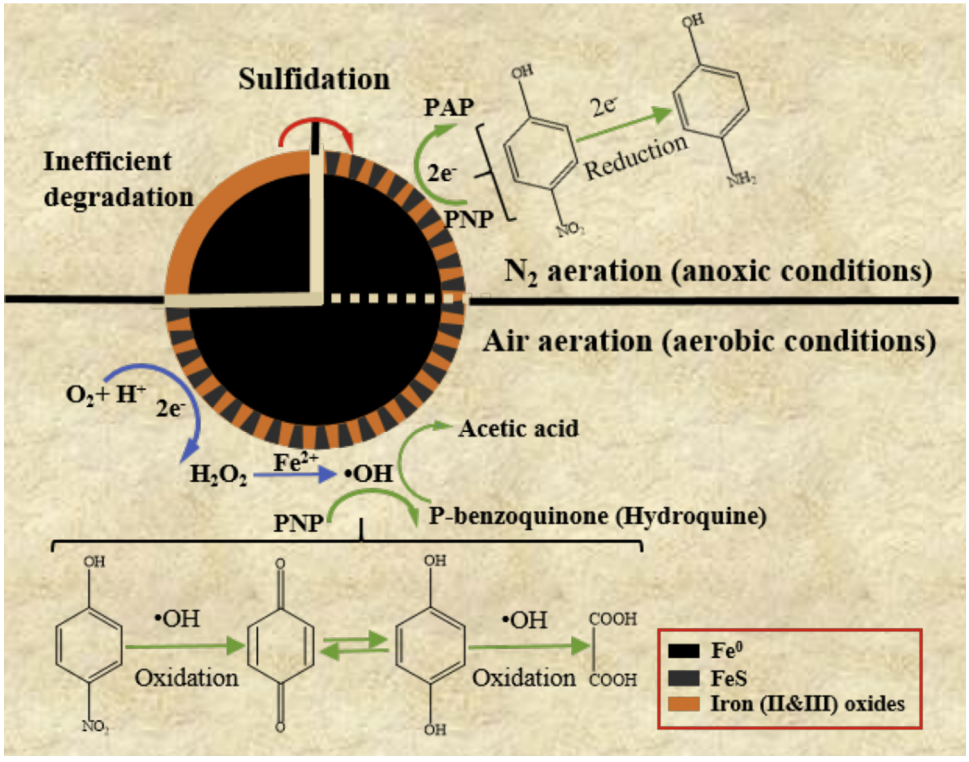

Fig. 11. Main degradation mechanisms for PNP in S-NZVI systems under aerobic or anoxic conditions.

3.7. Proposed pathway for PNP degradation under anoxic and aerobic conditions

To clarify primary mechanisms for PNP degradation in S-NZVI systems under anoxic and aerobic conditions, various intermediates in treatment effluents after 60 min reaction from different systems were detected by GC–MS, and these results are shown in Fig. 9. The dominating intermediates (*p*-aminophenol, *p*-benzoquinone and hydroquinone) and a small quantity of acetic acid appeared in the effluent treated under aerobic conditions, whereas in the effluent treated under anoxic conditions, the identified degradation products included *p*-aminophenol and a small amount of *p*-benzoquinone. In order to confirm the results, we detected the concentrations of main intermediates (*p*-aminophenol standing for reduction products and *p*-benzoquinone standing for oxidation products) shown in Fig. 10. Under aerobic conditions, the concentration of *p*-aminophenol rose in the first stage, and then decreased. However, the main product was *p*-aminophenol under anoxic conditions. The phenomena indicated that the PNP degradation process under aerobic conditions could be regarded as an oxidation combined with a reduction, while the main degradation process under anoxic conditions was regarded as a reduction. In Fig. 9, the presence of degradation product acetic acid, confirmed that the ring opening reaction occurred under aerobic conditions. In accordance with the conclusion in Section 3.6, the confirmation of trace amounts of *p*-benzoquinone in Figs. 9 and 10 also verified slight oxidation by •OH radicals proceeded in anoxic systems.

Based on aforementioned discussion and previous studies [10], the main PNP degradation mechanisms in S-NZVI systems were proposed in Fig. 11. First of all, the sulfidated S-NZVI utilized electron transfers more effectively to degrade PNP than NZVI. Hence, the degradation process could be accelerated by sulfidated systems. As shown in Fig. 11, under aerobic conditions, the PNP degradation process could be regarded as an oxidation combined with a reduction. Specifically, the DO was reduced into H_2O_2 by Fe(0) through two-electron reaction (Equation (1) and (2)) [25], and then H_2O_2 would be transferred into •OH radicals by the Fe^{2+} catalysis (Equation (3)). Then, the generated •OH radicals oxidized PNP into *p*-benzoquinone and its derivative, hydroquinone [10]. After that, the ring opening reaction occurred because of oxidation by enough •OH radicals, and acetic acid was presented in the effluent finally. The reduction process which was the same as that shown in anoxic conditions in Fig. 11 was not shown in aerobic conditions. However, under anoxic conditions, the vast majority of PNP was directly reduced to *p*-aminophenol. Additionally, the inconspicuous similar oxidation occurred and resulted in the formation of *p*-benzoquinine deriving from PNP or *p*-aminophenol [10], which was not shown in Fig. 11.

4. Conclusions

Taken together, addition of Na_2S in adequate concentration with the molar ratio of Na_2S to NZVI as 6.9 made surface coating by FeS, which results in increased reactivity towards PNP. The hydrophobic FeS layer acts as selective electron donor, which transfers electrons from the electron-rich Fe(0) core to PNP on the S-NZVI surface than the iron (hydr)oxide layer on the pristine NZVI surface. Particularly, the peak value of PNP apparent rate constants, calculated by the pseudo first-order kinetics equation, appeared at pH 7.60 in the pH range of 6.77-9.11 in the S-NZVI system under anoxic conditions, but shifted to pH 6.77 in the S-NZVI system under aerobic conditions and in NZVI systems with different conditions. It implies anoxic S-NZVI systems preferred to weaker alkaline solutions, while aerobic S-NZVI systems performed better in acidic solutions as well as NZVI systems. Due to the oxidation by •OH radicals, the highest efficiency of TOC removal reached 17.59% in the S-NZVI system at pH 6.77 under aerobic conditions. These results indicate that the aerobic treatment boosts the thorough degradation especially in slightly acidic conditions. Furthermore, the degradation process of PNP was analyzed by FTIR, XPS, capture of active species tests and GC–MS. Under aerobic conditions in S-NZVI systems, the formation of identified acetic acid, as a nontoxic ring opening by-product, confirms that the S-NZVI system could be a promising process with lower cost for toxic refractory industrial wastewater.

Considering cost-effectiveness and environmental safety, S-NZVI may be a more suitable alternative to NZVI modified with noble metal for enhanced reactivity. Sulfide ions present in wastewaters may enhance the reactivity of NZVI. However, their role in enhancing the reactivity of NZVI should be further investigated.

Acknowledgements

The study was financially supported by the National Program for Support of Top-Notch Young Professionals of China (2012), Projects 51222805, 51579096, 51521006 and 51508175 supported by National Natural Science Foundation of China, and the Program for New Century Excellent Talents in University from the Ministry of Education of China (NCET–11–0129).

Appendix A. Supplementary data

Supplementary data associated with this article can be found, in the online version, at http://dx.doi.org/10.1016/j.jhazmat.2016.07.042.

References

[1] R. Rangsivek, M.R. Jekel, Removal of dissolved metals by zero-valent iron (ZVI): Kinetics, equilibria, processes and implications for stormwater runoff treatment, Water Res. 39 (2005) 4153–4163.
[2] W. Yin, J. Wu, P. Li, X. Wang, N. Zhu, P. Wu, B. Yang, Experimental study of zero-valent iron induced nitrobenzene reduction in groundwater: the effects of pH, iron dosage, oxygen and common dissolved anions, Chem. Eng. J. 184 (2012) 198–204.
[3] W.A. Arnold, A.L. Roberts, Pathways and kinetics of chlorinated ethylene and chlorinated acetylene reaction with Fe(0) particles, Environ. Sci. Technol. 34 (2000) 1794–1805.
[4] Z. Xiong, B. Lai, P. Yang, Y. Zhou, J. Wang, S. Fang, Comparative study on the reactivity of Fe/Cu bimetallic particles and zero valent iron (ZVI) under different conditions of N_2, air or without aeration, J. Hazard. Mater. 297 (2015) 261–268.
[5] S.-H. Chang, S.-H. Chuang, H.-C. Li, H.-H. Liang, L.-C. Huang, Comparative study on the degradation of I.C. Remazol Brilliant Blue R and I.C. Acid Black 1 by Fenton oxidation and Fe-0/air process and toxicity evaluation, J. Hazard. Mater. 166 (2009) 1279–1288.
[6] S.-H. Chang, K.-S. Wang, S.-J. Chao, T.-H. Peng, L.-C. Huang, Degradation of azo and anthraquinone dyes by a low-cost Fe-0/air process, J. Hazard. Mater. 166 (2009) 1127–1133.
[7] J. Filip, F. Karlický, Z. Marušák, P. Lazar, M. Černík, M. Otyepka, R. Zbořil, Anaerobic reaction of nanoscale zerovalent iron with water: mechanism and kinetics, J. Phys. Chem. C 118 (2014) 13817–13825.
[8] D.H. Bremner, A.E. Burgess, D. Houllemare, K.-C. Namkung, Phenol degradation using hydroxyl radicals generated from zero-valent iron and hydrogen peroxide, Appl. Catal. B: Environ. 63 (2006) 15–19.
[9] C.R. Keenan, D.L. Sedlak, Factors affecting the yield of oxidants from the reaction of nanoparticulate zero-valent iron and oxygen, Environ. Sci. Technol. 42 (2008) 1262–1267.
[10] L. Tang, J. Tang, G. Zeng, G. Yang, X. Xie, Y. Zhou, Y. Pang, Y. Fang, J. Wang, W. Xiong, Rapid reductive degradation of aqueous p-nitrophenol using nanoscale zero-valent iron particles immobilized on mesoporous silica with enhanced antioxidation effect, Appl. Surf. Sci. 333 (2015) 220–228.
[11] X. Sun, Y. Yan, J. Li, W. Han, L. Wang, SBA-15-incorporated nanoscale zero-valent iron particles for chromium(VI) removal from groundwater: mechanism, effect of pH, humic acid and sustained reactivity, J. Hazard. Mater. 266 (2014) 26–33.

[12] D. O'Carroll, B. Sleep, M. Krol, H. Boparai, C. Kocur, Nanoscale zero valent iron and bimetallic particles for contaminated site remediation, Adv. Water Resour. 51 (2013) 104–122.
[13] W.-X. Zhang, C.-B. Wang, H.-L. Lien, Treatment of chlorinated organic contaminants with nanoscale bimetallic particles, Catal. Today 40 (1998) 387–395.
[14] Z. Liu, C. Gu, M. Ye, Y. Bian, Y. Cheng, F. Wang, X. Yang, Y. Song, X. Jiang, Debromination of polybrominated diphenyl ethers by attapulgite-supported Fe/Ni bimetallic nanoparticles: influencing factors, kinetics and mechanism, J. Hazard. Mater. 298 (2015) 328–337.
[15] B. Lai, Y. Zhang, Z. Chen, P. Yang, Y. Zhou, J. Wang, Removal of p-nitrophenol (PNP) in aqueous solution by the micron-scale iron–copper (Fe/Cu) bimetallic particles, Appl. Catal. B: Environ. 144 (2014) 816–830.
[16] P. Guo, L. Tang, J. Tang, G. Zeng, B. Huang, H. Dong, Y. Zhang, Y. Zhou, Y. Deng, L. Ma, S. Tan, Catalytic reduction-adsorption for removal of p-nitrophenol and its conversion p-aminophenol from water by gold nanoparticles supported on oxidized mesoporous carbon, J. Colloid Interface Sci. 469 (2016) 78–85.
[17] Y. Zhou, L. Tang, G. Yang, G. Zeng, Y. Deng, B. Huang, Y. Cai, J. Tang, J. Wang, Y. Wu, Phosphorus-doped ordered mesoporous carbons embedded with Pd/Fe bimetal nanoparticles for the dechlorination of 2,4-dichlorophenol, Catal. Sci. Technol. 6 (2016) 1930–1939.
[18] E.-J. Kim, J.-H. Kim, A.-M. Azad, Y.-S. Chang, Facile synthesis and characterization of Fe/FeS nanoparticles for environmental applications, ACS Appl. Mater. Interface 3 (2011) 1457–1462.
[19] S.R. Rajajayavel, S. Ghoshal, Enhanced reductive dechlorination of trichloroethylene by sulfidated nanoscale zerovalent iron, Water Res. 78 (2015) 144–153.
[20] D. Fan, R.P. Anitori, B.M. Tebo, P.G. Tratnyek, J.S. Lezama Pacheco, R.K. Kukkadapu, M.H. Engelhard, M.E. Bowden, L. Kovarik, B.W. Arey, Reductive sequestration of pertechnetate ($^{99}TcO_4^-$) by nano zerovalent iron (nZVI) transformed by abiotic sulfide, Environ. Sci. Technol. 47 (2013) 5302–5310.
[21] S.-W. Park, S.-K. Kim, J.-B. Kim, S.-W. Choi, H.I. Inyang, S. Tokunaga, Particle surface hydrophobicity and the dechlorination of chloro-compounds by iron sulfides, Wat. Air Soil Pollut. Focus 6 (2006) 97–110.
[22] E.J. Kim, K. Murugesan, J.H. Kim, P.G. Tratnyek, Y.S. Chang, Remediation of trichloroethylene by feS-coated iron nanoparticles in simulated and real groundwater: effects of water chemistry, Ind. Eng. Chem. Res. 52 (2013) 9343–9350.
[23] E.C. Butler, K.F. Hayes, Factors influencing rates and products in the transformation of trichloroethylene by iron sulfide and iron metal, Environ. Sci. Technol. 35 (2001) 3884–3891.
[24] C. He, J. Yang, L. Zhu, Q. Zhang, W. Liao, S. Liu, Y. Liao, M. Abou Asi, D. Shu, pH-dependent degradation of acid orange II by zero-valent iron in presence of oxygen, Sep. Purif. Technol. 117 (2013) 59–68.
[25] I.A. Katsoyiannis, T. Ruettimann, S.J. Hug, pH dependence of fenton reagent generation and As(III) oxidation and removal by corrosion of zero valent iron in aerated water, Environ. Sci. Technol. 42 (2008) 7424–7430.
[26] S.H. Joo, A.J. Feitz, T.D. Waite, Oxidative degradation of the carbothioate herbicide, molinate using nanoscale zero-valent iron, Environ. Sci. Technol. 38 (2004) 2242–2247.
[27] C.E. Noradoun, I.F. Cheng, EDTA degradation induced by oxygen activation in a zerovalent iron/air/water system, Environ. Sci. Technol. 39 (2005) 7158–7163.
[28] C.P. Adams, K.A. Walker, S.O. Obare, K.M. Docherty, Size-dependent antimicrobial effects of novel palladium nanoparticles, PLoS One 9 (2014) e85981.
[29] M. Murugananthan, G.B. Raju, S. Prabhakar, Removal of sulfide, sulfate and sulfite ions by electro coagulation, J. Hazard. Mater. 109 (2004) 37–44.
[30] B. Lai, Z. Chen, Y. Zhou, P. Yang, J. Wang, Z. Chen, Removal of high concentration p-nitrophenol in aqueous solution by zero valent iron with ultrasonic irradiation (US–ZVI), J. Hazard. Mater. 250–251 (250) (2013) 220–228.
[31] T. Wang, N. Lu, J. Li, Y. Wu, Y. Su, Enhanced degradation of p-nitrophenol in soil in a pulsed discharge plasma-catalytic system, J. Hazard. Mater. 195 (2011) 276–280.
[32] Y. Zhang, N. Yang, M. Murugananthan, S. Yoshihara, Electrochemical degradation of PNP at boron-doped diamond and platinum electrodes, J. Hazard. Mater. 244–245 (244) (2013) 295–-.
[33] L. Wang, K. Daub, Z. Qin, J.C. Wren, Effect of dissolved ferrous iron on oxide film formation on carbon steel, Electrochim. Acta 76 (2012) 208–217.
[34] J.T. Nurmi, P.G. Tratnyek, V. Sarathy, D.R. Baer, J.E. Amonette, K. Pecher, C. Wang, J.C. Linehan, D.W. Matson, R.L. Penn, M.D. Driessen, Characterization and properties of metallic iron nanoparticles: spectroscopy, electrochemistry, and kinetics, Environ. Sci. Technol. 39 (2005) 1221–1230.
[35] W. Lee, B. Batchelor, Abiotic reductive dechlorination of chlorinated ethylenes by iron-bearing soil minerals. 1. Pyrite and magnetite, Environ. Sci. Technol. 36 (2002) 5147–5154.
[36] Y. Xiao, M.R. Wiesner, Characterization of surface hydrophobicity of engineered nanoparticles, J. Hazard. Mater. 215-216 (2012) 146–151.
[37] D. Tang, Z. Zheng, K. Lin, J. Luan, J. Zhang, Adsorption of p-nitrophenol from aqueous solutions onto activated carbon fiber, J. Hazard. Mater. 143 (2007) 49–56.
[38] L. Tang, G. Yang, G.-M. Zeng, Y. Cai, S. Li, Y. Zhou, Y. Pang, Y. Liu, Y. Zhang, B. Luna, Synergistic effect of iron doped ordered mesoporous carbon on adsorption-coupled reduction of hexavalent chromium and the relative mechanism study, Chem. Eng. J. 239 (2014) 114–122.
[39] Z. Droussi, V. D'orazio, M.R. Provenzano, M. Hafidi, A. Ouatmane, Study of the biodegradation and transformation of olive-mill residues during composting using FTIR spectroscopy and differential scanning calorimetry, J. Hazard. Mater. 164 (2009) 1281–1285.
[40] L. Tang, J. Wang, G. Zeng, Y. Liu, Y. Deng, Y. Zhou, J. Tang, J. Wang, Z. Guo, Enhanced photocatalytic degradation of norfloxacin in aqueous Bi_2WO_6 dispersions contaning nonionic surfactant under visible light irradiation, J. Hazard. Mater 306 (2016) 295–304.
[41] M. Mullet, S. Boursiquot, M. Abdelmoula, J.-M. Génin, J.-J. Ehrhardt, Surface chemistry and structural properties of mackinawite prepared by reaction of sulfide ions with metallic iron, Geochim. Cosmochim. Acta 66 (2002) 829–836.
[42] W. Yan, A.A. Herzing, C.J. Kiely, W.X. Zhang, Nanoscale zero-valent iron (nZVI): aspects of the core-shell structure and reactions with inorganic species in water, J. Contam. Hydrol. 118 (2010) 96–104.
[43] N. Andreu, D. Flahaut, R. Dedryvère, M. Minvielle, H. Martinez, D. Gonbeau, XPS investigation of surface reactivity of electrode materials: effect of the transition metal, ACS Appl. Mater. Interface 7 (2015) 6629–6636.
[44] M. Mullet, S. Boursiquot, J.-J. Ehrhardt, Removal of hexavalent chromium from solutions by mackinawite, tetragonal FeS, Colloid Surf. A 244 (2004) 77–85.
[45] T. Wang, G. Qu, Q. Sun, D. Liang, S. Hu, Evaluation of the potential of p-nitrophenol degradation in dredged sediment by pulsed discharge plasma, Water Res. 84 (2015) 18–24.
[46] X. Zhang, G. Li, Y. Wang, J. Qu, Microwave electrodeless lamp photolytic degradation of acid orange 7, J. Photochem. Photobiol. A 184 (2006) 26–33.